Scientific Research Publishing

Open Journal of Civil Engineering, 2025, 15(4), 710-727
https://www.scirp.org/journal/ojce
ISSN Online: 2164-3172
ISSN Print: 2164-3164

Effect of Segregation on the Performance of 0/31.5 Granular Materials from the Kombe Deposit Used in Road Construction

Sylvain Ndinga Okina[1,2]*, Alain Symphorien Ndongo[1], Adoum Waibaye[3], Prince Mang Egrik W. O. Nkembo[1], Arsene Joseph Bockou Ekockaut[1,2], Louis Ahouet[1,2,4]

[1]Higher National Polytechnic School (ENSP), Marien Ngouabi University, Brazzaville, Congo
[2]Higher Institute of Architecture, Urbanism, Building and Public Works, Denis Sassou Nguesso University, Brazzaville, Congo
[3]Higher National School of Public Works (ENSTP), N'Djamena, Tchad
[4]Control Office for Building and Publics Works (BCBTP), Brazzaville, Congo
Email: *sylvain.ndingaokina@umng.cg

How to cite this paper: Okina, N.S., Ndongo, A.S., Waibaye, A., Mang, N.P.E.W.O., Ekockaut, A.J.B. and Ahouet, L. (2025) Effect of Segregation on the Performance of 0/31.5 Granular Materials from the Kombe Deposit Used in Road Construction. *Open Journal of Civil Engineering*, **15**, 710-727.
https://doi.org/10.4236/ojce.2025.154038

Received: September 29, 2025
Accepted: October 31, 2025
Published: November 3, 2025

Abstract

The segregation of different particle sizes in a granular mixture leads to performance defects in construction materials. This article analyses the segregation of 0/31.5 crushed aggregates from the Kombe quarry used in road construction in Congo. The methodology consists of taking samples using various laboratory and field techniques (PD, DL, SCS, SCB, Q) likely to cause segregation. Data modeling using OriginPro2019b software consisted of deriving theoretical models to control segregation. The results obtained from the analysis of the descriptors of the particle size distribution curves ($Cu > 2$, $Cc < 1$; $Cc > 3$) and the fineness modulus (5% and 45%) show that the material studied is prone to granular segregation. The DL sampling model, with 44.54% fines and 37.16% gravel, corresponds well to the normative particle size distribution and appears to be the best for mitigating the effects of segregation. The theoretical DL model obtained by modeling gives an optimal granular composition, with 13.43% fine sand, 31.03% coarse sand, 37.16% gravel and 18.36% stones. The high percentages of fine elements in the material result in a 3.04% decrease in dry density for the SCB ($Ds = 2.238\ g/cm^3$) and Q ($Ds = 2.170\ g/cm^3$) samples. The SCB model has a high CBR (158.5%), indicating a mechanical improvement in the material. The presence of a granular class resulting from segregation affects the compactness of the material layer.

Keywords

Granular Segregation, Material Sampling, Compactness, Intergranular Porosity, Segregation Particle Size Distribution

1. Introduction

Granular materials are known for their variable density, shapes and diameters. The grains that make up these materials generally lose energy when interacting with other moving particles, which often leads to granular segregation [1]-[3]. The spillage of granular materials during stacking and their flow into silos often causes grain sorting. The resulting segregation and stratification are responsible for heterogeneous distributions among granular samples during and after deposition. The disparity in such distributions in granular mixtures is mainly explained by changes in physical and mechanical properties [4]-[7]. The segregation of the granular particle used in the concrete or road construction industry is a major problem affecting the mechanical behavior of base layers in pavements [8]-[11]. The segregation of granular mixtures influences the stability of the E/C ratio during concrete formulation, while the size of the aggregates has a significant impact on mechanical strength [8] [11]. The repeated application of varying traffic loads or the compaction of pavement layers causes attrition in roads, which produces more or less plastic fines that alter the material's particle size distribution and mechanical behavior over time [12] [13]. The segregation of crushed aggregate is often ignored or poorly taken into account during adjustments in quarries or on road construction sites, which generally affects the quality of the infrastructure over time. Hydzik-WiśniewskaL *et al.* 2018 [14] showed that the grain content of crushed aggregates 0/31.5 and 0/63 has a considerable influence on the CBR bearing ratio. Wu *et al.* 2019 [15] concluded that, depending on the levels of granular segregation, the air voids in mineral aggregates (VMA) gradually decrease, the number of contact points between particles increases significantly, and the contact forces gradually decrease, and the segregation of coarse aggregates has a more significant effect on the load resistance. The mechanisms behind the segregation of granular materials used in road construction can be explained by the nature and production method of the materials and the conditions under which they are used. **Figure 1** illustrates some sources of segregation of granular materials caused during use on different compaction sites.

Figure 1. Use of granular materials in road pavement and segregation phenomena.

Despite technical recommendations to prevent granular segregation in road works [16], the mechanisms of granular material segregation are not fully understood. To our knowledge, there is no unified model available to define, quantify and control the segregation of crushed aggregate in practice. The objective of this study is to evaluate, based on laboratory testing and modeling, the effects of segregation on the physical and mechanical properties of 0/31.5 mm crushed aggregate used in a layer road. The idea is to find the particle size distribution of the material that lacks certain grain sizes but offers better compactness and good load-bearing capacity. The derivation of a theoretical model on this basis aims to control the segregation of granular mixtures.

2. Materials and Method

2.1. Materials

The material studied is crushed 0/31.5 aggregate from Inkissi sandstone in Kombe located south of Brazzaville on the banks of the Congo River (Figure 2). Its bulk density, specific weight and Los Angeles coefficient were determined in the Civil Engineering Laboratory of the Higher Polytechnic National School (ENSP) at Marien Ngouabi University.

Figure 2. Location of the deposit, sample of 0/31.5 mm aggregate.

OriginPro2019b software is designed to generate interactive 2D and 3D graphs and analyze data. Data analysis in Origin includes statistics, signal processing, curve fitting and peak analysis. Origin's curve fitting is performed by a non-linear least squares fitter based on the Levenberg-Marquardt algorithm. Various scientific studies on geotechnics and the study of construction materials have been successfully carried out using OriginPro2019b [17].

2.2. Methods

Procedure for developing the segregation mechanism

Five 05 samples of 0/31.5 mm aggregate (PD, DL, SCS, SCB, Q) taken using specific sampling methods were subjected to a series of physical and mechanical tests. Four standardized samples were taken in accordance with the standard (EN 932-1) [18] and one sample was taken directly from the bulk sample, as is done on construction sites and in laboratories. The particle size analysis of dry material samples subjected to vibration made it possible to quantify segregation. Modified Proctor test and CBR test were used to assess the mechanical effects induced by segregation under vibration of the material. For each sample, checks based on the tests (compactness, granular spindles, fineness modulus, bearing capacity) were carried out to verify the degree of segregation in the material.

Modeling segregation control equations

Modeling of segregation control equations is performed using the ANOVA calculation model (OriginPro2019b), which generates various multiple linear regression equations to model optimal particle size distribution curves. ANOVA model analysis is an analysis of variance, which is a set of statistical models used to verify whether the means of the groups come from the same population. Using this model (ANOVA) provides more smoothing points for the curve, allowing for a more accurate assessment of the fit, due to the large number of particles of different sizes in granular materials [19].

For a given sample ($Y_i, X_{i1}, \cdots, X_{ip}$) $i \in \{1, n\}$, it is necessary to explain as precisely as possible the values taken by Y_i, known as the endogenous variable, based on a series of explanatory variables $X_{i1}, \cdots, X_{ip}$. The theoretical model, formulated in terms of random variables, is generated in the following form (1):

$$Y = a_0 + a_1 X_{i1} + a_2 X_{i2} + \cdots + a_p X_{ip} + \varepsilon_i, \; i = 1, \cdots, n \tag{1}$$

where ε_i is the model error that expresses or summarizes the information missing from the linear explanation of the values of Y_i based on $X_{i1}, \cdots, X_{ip}$ (specification problem, variables not taken into account…). The coefficients $a_0, a_1, \cdots, a_p$ are the parameters to be estimated.

Figures 3-7 illustrate some of the experimental steps involved in analyzing material samples in the laboratory. Figure 3 shows the tested 0/31.5 aggregate sample and the schematic cone composition of the separated aggregates.

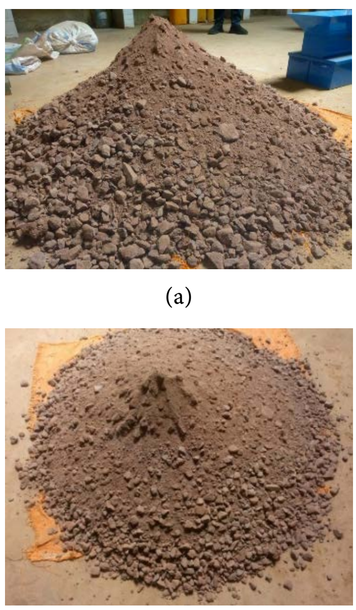

(a)

(b)

Figure 3. (a) TVC-0/31.5 sample, (b) schematic conical composition of segregated aggregates.

Figure 4. Preparation of material samples by quartering.

(a) (b)

Figure 5. (a) Refusal, (b) passing at grain size.

Figure 6. Measurement of the bulk density of 0/31.5 aggregate.

Figure 7. CBR test on 0/31.5 aggregate.

Figure 3 shows the stockpile formed beforehand (**Figure 3(a)**) and the segregation resulting from the unloading of material from a fixed conveyor (**Figure 3(b)**). This is suitable for sampling based on the actual state of segregation. It explains the causes of segregation during material handling. The core at the top of the pile forms a cone made up of fine particles, while the material spilling out on either side of the core consists of medium-sized particles resting on the coarse particles forming triangles at the base [7] [20] [21]. **Figure 4** shows the process of material preparation by manual and standardized sampling.

Parameters of tested materials

The particle size distribution, characterized by grain diameter, shape and coefficients of uniformity and curvature, allows the nature of the material to be defined in accordance with standards NF P 94-056 and EN 933-2 [22] [23]. Five samples (PD, DL, SCS, SCB, Q) were analyzed on 22 sieves with diameters ranging from Dmax (31.5 mm) to d (0.08 mm). The particle size distribution curve is obtained from sieve analysis values (**Figure 5**). Sieve analysis expresses the quantity of material that passes through a set of sieves and is determined by the following formula:

$$\%P = 100\% - \%R \tag{2}$$

$$\%R = \frac{MR}{MT} * 100 \tag{3}$$

P: passing; R: refusal; MR: cumulative rejection mass; MT: total dry mass.

The uniformity (Cu) and curvature (Cc) coefficients help to analyze the particle size distribution curve obtained on the basis of the sieve diameter ratios, where Dx is the grain size corresponding to x % by weight of sieved material:

$$Cu = \frac{D60}{D10} \tag{4}$$

$$Cc = \frac{(D30)^2}{D10 \times D60} \tag{5}$$

The apparent density determines, in accordance with standard NF EN 1097-3 [24], the density of the material before compaction or manufacture. It corresponds to the ratio between the mass of the dry aggregate and the volume it occupies without compaction in a metal mould, including the volume of intergranular voids (**Figure 6**).

The bulk density or apparent density ρ_b (T/m³) is calculated using the following formula:

$$\rho_b = \frac{\text{m2} - \text{m1}}{V} \quad (6)$$

where: V is the volume of the container (l);

M1: mass of the mould and sample (kg)

M2: mass of the empty mould (kg)

Intergranular porosity γ corresponds to the percentage of intergranular voids in the container; it is calculated using the following equation:

$$\gamma = \frac{\rho_p - \rho_b}{\rho_p} \quad (7)$$

where ρ_p is the actual density in T/m³, determined in accordance with standard EN 1097-6 [25].

The modified Proctor was measured on samples of material compacted in a standardized mould at a conventional energy level in accordance with standard NF P94-093 [26]. The material tested is characterised by the maximum dry Proctor density (γdmax) corresponding to an optimum water content (W_{OPM}).

The CBR (California Bearing Ratio) test measures the bearing capacity of the material or soil that has undergone prior compaction energy in accordance with the standard (NF P94-078, NF EN 13286-47) [27] [28]. The bearing capacity of the material is characterized by the CBR index calculated during the punching of the test specimen after 4 days of immersion (**Figure 7**). The index sought is conventionally defined as the greater of the two ratios calculated as follows:

$$\text{CBR1} = \frac{100 * F_{2.5\text{mm}}}{13.35}; \quad \text{CBR2} = \frac{100 * F_{5\text{mm}}}{19.93} \quad (8)$$

where F is the force exerted by the piston to drive it into the test piece (kN).

3. Results and Discussion

3.1. Experimental Characteristics

Analysis of the effect of segregation on the particle size distribution of crushed aggregate

Figure 8 shows the particle size distribution curves obtained from the five samples.

In **Figure 8**, the PD, DL, SCS and Q curves approach the upper range, while the DL and SCB curves are entirely within the granular reference ranges (CEBTP, 84; EN 13285) [29] [30]. This range incorporates a relationship between the particle size distribution and the mechanical strength of the material (Los Angeles coefficient, LA ≤ 45; Micro-Deval coefficient, MDE ≤ 35), which takes into account the effects of compaction on the bearing capacity. Key upper and lower limit percentages are, for example, sieve (min; max): 0.5 mm (5; 85%); 2 mm (16; 47%)…16 mm (55; 85%). The SCB curve also approaches the lower limit of the range.

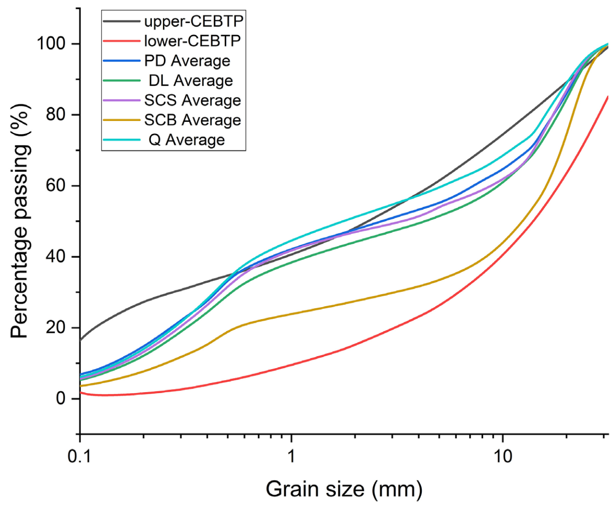

Figure 8. Grain size curves for crushed aggregate samples 0/31.5.

The particle size analyses by quartering of the materials show the greatest deviation from the reference ranges (Q curve). The deviation zone of the particle size curves is in the same interval between the sieve openings of 0.5 and 4 mm. The extremes are those of the quartering between coarse sand and gravel (0.5 mm and 4 mm). For PD, SCS and DL, the deviation from the reference range only occurs between the 0.5 mm and 2 mm sieves, which correspond to the coarse sand zone (**Table 1**). The SCB curve shows that the material lacks coarse sand and does not come out of the pin; it generates granular segregation relative to the overall appearance of all the curves and does not represent the general nature of the sample. The 0/31.5 aggregate studied, despite its high gravel content, consists entirely of coarse sand with a fineness modulus (Mf) between 5% and 45%. Among all the curves obtained, the material is characterized by a spread or varied grain size (Cu > 2), but poorly calibrated (Cc < 1 and Cc > 3). Consequently, this material is prone to segregation phenomena.

Table 1. Granulometric indicators Cu, Cc, Mf and % P.

Parameters	Sample				
	PD	DL	SCS	SCB	Q
Mf (%)-0.5 mm sieve	29.4	29.3	31.6	19.2	33.9
Cu	63.3	45	43.8	63.7	31.8
Cc	0.2	0.2	0.1	4	0.3
% P					
% fine sand (0.02 - 0.2 mm)	16.64	13.79	15.06	8.25	16.07
% coarse sand (0.2 - 2 mm)	31.86	30.74	32.39	19.29	35.87
% gravel (2 - 20 mm)	34.91	37.16	35.16	44.81	33.65
% pebbles (>20 mm)	16.59	18.31	17.38	27.64	14.41

In terms of sampling methodology, the curves show that the PD (16.64%) and Q (16.07%) models favor the collection of fine elements during sampling. These results are similar to those obtained when sampling at the top of the cone stock (15%), which is an anomaly for the overall representation of the sample.

The SCB curve at the base of the conical stock contains fewer fine elements (8.25%) than the others; it is rich in gravel and pebbles (44.81% and 27.64% respectively), and therefore has a high proportion of coarse elements. The DL curve contains the median values for fines, *i.e.* 13.79%. All the curves obtained model the possibility of granular segregation linked to the handling of the material. The SCB curve strongly represents the phenomenon of segregation in a granular mass compared to the initial sample. Table 1 lists the values of the Cu, Cc and Mf coefficients and the proportions of minerals constituting the material on a 5 mm sieve.

The bulk density of the* 0/31.5 *aggregate

The average apparent density of each sample tested varies between 1.790 and 1.920 g/cm^3. The lowest densities were obtained from the sample taken by quartering Q (1.790 g/cm^3), while the highest values were obtained from direct sampling PD (1.920 g/cm^3) and at the top of the conical stockpile SCS (1.915 g/cm^3). The density values obtained are higher than the average density obtained for Kombe sandstone, which is approximately 1.400 g/cm^3 for coarse elements [31]. This can be explained by the presence of crushed sand in the 0/31.5 aggregate. The apparent density values and intergranular porosity calculated using a specific weight γ of 2.630 g/cm^3 are shown in Table 2.

Table 2. Physical parameters of crushed aggregate 0/31.5.

Parameters	Sample				
	PD	DL	SCS	SCB	Q
ρ_b (g/cm^3)	1.920	1.895	1.915	1.872	1.790
ρ_P (g/cm^3)	2.630	2.630	2.630	2.630	2.630
γ (%) = $(\rho_P - \rho_b)/\rho_P$	27.00	27.95	27.19	28.82	31.94
γ_{moy} (%)			28.58		

ρb-bulk density; ρp-specific weight; γ-intergranular porosity.

***Effect of segregation on the compaction of crushed aggregate* 0/31.5**

Figure 9 shows the modified Proctor curves for the samples tested.

Figure 9 shows that, depending on the shape, maximum moisture content and position, the PD curve shifts to the left relative to the others, with the material behaving like silty clay, with a maximum dry density γdmax (2.20 g/cm^3) and an optimum water content W_{OPM} (5.17%); The same applies to the SCS curve, whose maximum dry density γdmax (2.18 g/cm^3) corresponds to an optimum water content W_{OPM} (6.96%). The compaction behavior of the SCB, DL and Q curves is similar to that of gravelly sand, with maximum dry densities γdmax and optimum water contents WOPM of (2.24 g/cm^3; 5.29%), (2.17 g/cm^3; 6.31%) and (2.17 g/cm^3; 6.76%). Based on this analysis, the dispersion of the PD curve indicates significant segregation of the mixture. However, the curves for the SCS, DL and Q samples, which have a rich composition in fine elements, show that these parts of the material require approximately 1.2% more water content for good compaction compared to the PD and SCB samples. The variability of these values for the same aggregate highlights the difficulty of obtaining similar granular compositions for each sample taken using different procedures. Table 3 provides information on the modified Proctor values obtained and their correction.

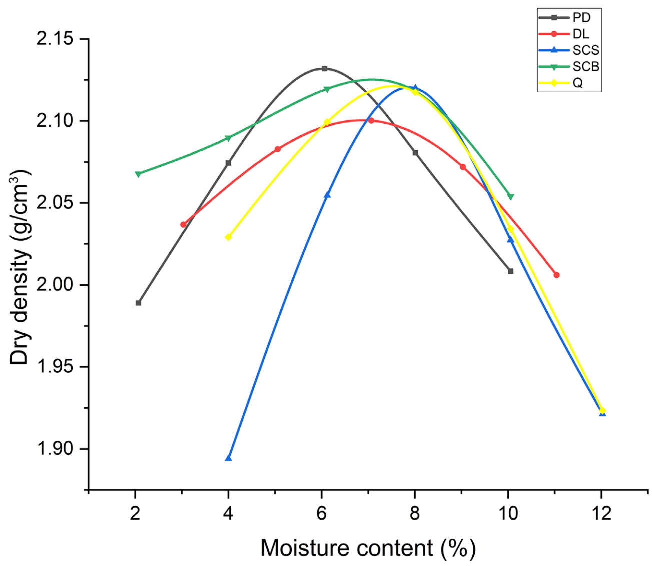

Figure 9. Modified proctor curves for 0/31.5 aggregate.

Table 3. Modified proctor properties of 0/31.5 aggregate.

Parameters	Sample				
	PD	DL	SCS	SCB	Q
γdmax (g/cm^3)	2.13	2.10	2.12	2.12	2.12
w_{OPM}	6.20	7.5	8.0	7.2	7.6
r (%)-20 mm sieve	16.57	15.94	13.04	26.54	11.06
ρ_P (g/cm^3)			2.630		
γdmax' (g/cm^3)	2.20	2.17	2.18	2.24	2.17
w_{OPM}' (%)	5.17	6.31	6.96	5.29	6.76

r(%)-rejects content on a 20 mm sieve.

Figure 10 models the influence of the percentage of fines (0.02 - 0.2 mm) on the dry density of the aggregate. Although the densities are within the same range (2.10 - 2.25 g/cm^3), it can nevertheless be seen that the presence of fine particles reduces the dry density by approximately 3.04%, if we consider the extremes for the SCB model (DD = 2.24 g/cm^3; fine sand = 27.57%) and the Q model (DD = 2.17 g/cm^3; fine sand = 51.94%). This clearly shows the effect of granular segregation on the compaction of materials, which means that the presence of a small or large granular fraction alters the compactness of road material layers. The curve forms a parabola with an extremum between the SCS and Q models, for which the maximum dry density would be 2.21 g/cm³ and the percentage of fine sand 49.6%. DL (DD = 2.20 g/cm³ and fine sand 48.5%) is the model that comes closest to the maximum density extremum, which shows that it is indeed the model that minimizes granular segregation.

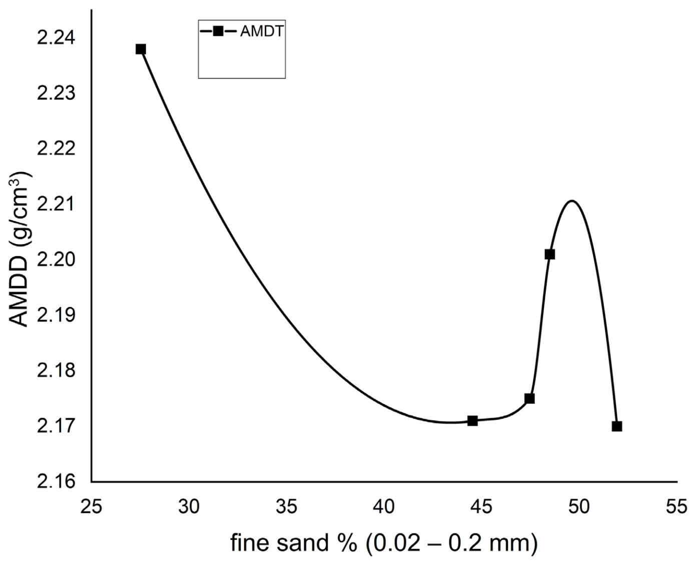

Figure 10. Influence of fines (0.02 - 0.2 mm) on Proctor dry density of all models. AMDD: average maximum dry density.

Effect of granular segregation on CBR bearing capacity

Figure 11 shows the penetration effort curves from the CBR test, and **Figure 12** shows the influence of the modified Proctor optimal dry density (OPM) on the bearing capacity of the material.

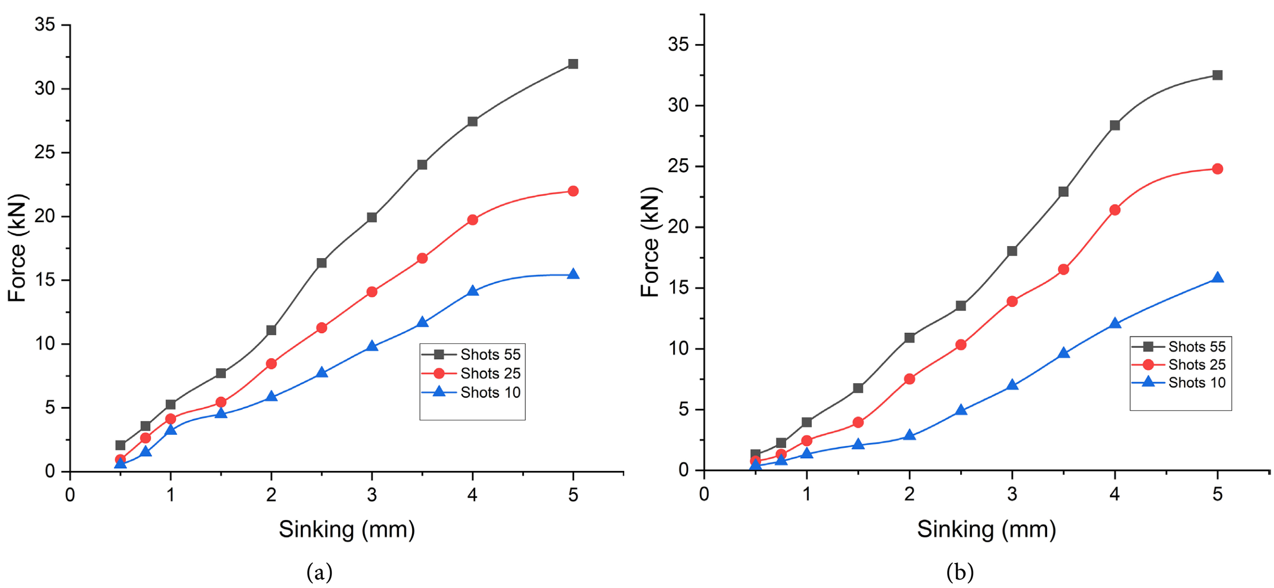

Figure 11. Model effort-penetration curves, (a) SCB, (b) SCS.

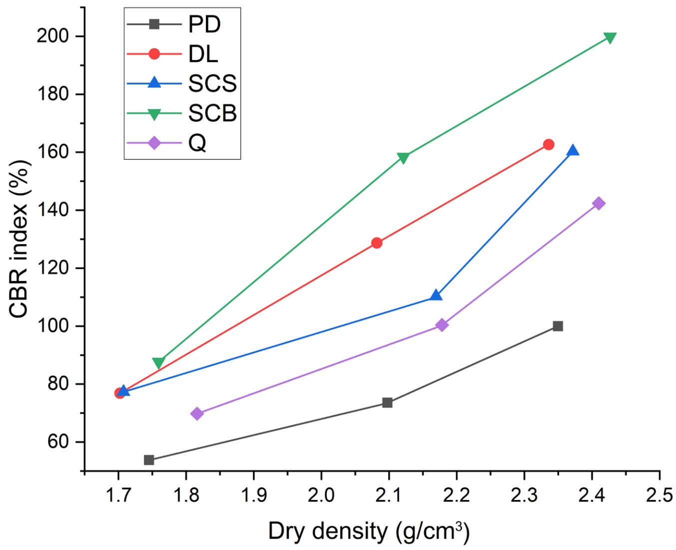

Figure 12. Influence of OPM dry density on the CBR index.

The average CBR and compactness values for the five samples are shown in **Table 4**.

Table 4. CBR at 95% OPM and compactness of samples.

Parameters	Sample				
	PD	DL	SCS	SCB	Q
γ_{CBR} (g/cm^3)	2.09	2.08	2.17	2.12	2.18
γdmax (g/cm^3)	2.13	2.10	2.12	2.12	2.12
C (%)	95.31	95.99	99.74	94.79	100.43
CBR (%)	73.5	129.75	103	158.5	90.6

C (%)-average compactness; γ_{CBR}-density of CBR.

The CBR values obtained in this study are significantly higher than those obtained in the work of Hydzik-Wiśniewska *et al.* (2018) on 0/31.5 crushed aggregates, for which the values vary between 22.4 and 40.3%. This may be related to the geological nature of the terrain, as the geology of a soil varies from one point to another. Based on the sampling method, the PD model has the lowest CBR values (69.5% and 73.5%). This model leads to significant segregation in terms of the implementation method. It is clear that the data (results) for this model are scattered, lack logic and do not follow the overall average representing the original sample. The Q model, which has a high percentage of fines (51.94%), also shows low CBR values (87% and 90.6%), as the sample behaves like gravelly sand. The SCB model has higher CBR values (137% and 158.5%). This is due to the high proportion of coarse particles (44.81%) in the sample. The SCS model taken from the top of the conical stockpile, rich in fines (47.46%), has low CBR values (99% and 103%) compared to the DL model, which continues to show median values

(117.2% and 129.75%) in all tests performed. The DL model therefore offers the best control of segregation in 0/31.5 granular materials.

Analysis of CBR test specimens for segregation

The water absorption test values for the CBR samples are recorded in **Table 5**. The absorption rates of the CBR samples show that the PD and Q samples with the lowest CBR values are those with the highest absorption rates (PD = 2.29% and Q = 1.27%). This is because the friction of sizes in a granular mixture is mainly affected by inter-particle forces, which decrease with water saturation and increased water pressure in the voids, resulting in a decrease in the bearing capacity of the material due to compaction effect [32]. However, there appears to be an inconsistency in the SCB test tube, which has a high imbibition rate but CBR values ranging from 137% to 158.5%. This inconsistency can be explained by intergranular porosity (**Table 2**). Without taking into account the PD model, which causes segregation in each of the samples, we can see that the imbibition rate follows that of intergranular porosity. The Q and SCB models, rich in fine and coarse elements respectively, behave as described in **Figure 8** as a limiting case of a perfect bimodal distribution. As a result, some models have voids that cannot be completely filled, creating high porosity in the stacking. The SCS model, which has lower imbibition values, is certainly the one where the grain arrangement is balanced in terms of compactness, *i.e.* the grains fill each other perfectly. Except that it does not represent the original granular spindle. It behaves like gravelly sand (fines = 47.46%). This is justified by low CBR values (99% and 103%) compared to the DL and SCB models. The DL model seems to best control segregation in the material. **Table 5** summarizes the imbibition analysis of the test specimens. The DL model appears to best control segregation in the material. **Table 5** summarizes the analysis of the imbibition of the test specimens.

Table 5. 96-hour saturation rate of CBR test specimens after compaction.

Parameters	Sample				
	PD	DL	SCS	SCB	Q
maV (g)	12,488	11,315	11,464	12,570	12,131
mAp (g)	12,594	11339.5	11,486	12,602	12,193
Me (g)	7858	7242	6596	7712	7264
Mc	4630	4818	4868	4858	4867
mWi	106	24.5	22	32	62
i (%)	**2.29**	0.51	0.45	0.66	1.27
γ (%)	**27.00**	27.95	27.19	28.82	31.94

maV—mass before immersion; mAp—mass after immersion; me—test specimen mass; mc—compacted material mass; mWi—water-soaked mass; i—average soak rate; γ—intergranular porosity.

3.2. Discussion

Segregation model simulation

Of the five sampling models studied, only the DL curve clearly models a granular material without significant segregation. Therefore, the modeling of the percentage of passers based on granular fractions is used to simulate a predictive model of segregation rates. Figure 13 shows the correlation between the percentage of passers and the granular fraction of the five models.

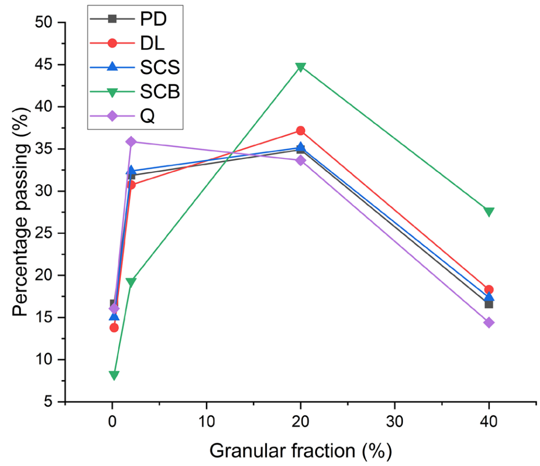

Figure 13. Correlation between the percentage of passers-by and granular fractions of the five models.

The SCB curve deviates completely from the others, and the Q curve deviates slightly between the granular fractions of 0 to 10 mm, confirming the assumptions of material segregation in these samples. Based on the ANOVA modeling of the PD, DL and SCS curves in OriginPro, we can see that these curves are well correlated and simulated, although the coefficient of determination (R^2) for all models is equal to 0.99. Figure 14 shows an illustration of the DL model simulation.

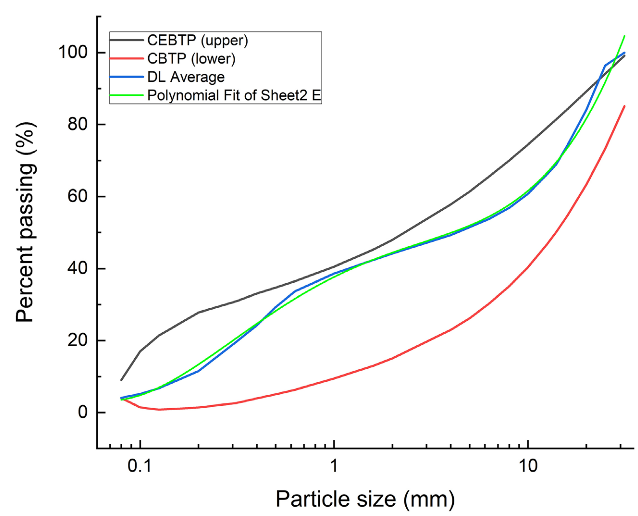

Figure 14. Modeling the particle size distribution curve of the DL model.

The overall segregation control equation obtained by ANOVA simulation and the associated index values are recorded in Table 6.

Table 6. Standard equations for the particle size distribution curves of the models studied.

Equation	$Y_i = I + B_1 * x^1 + B_2 * x^2 + B_3 * x^3 + B_4 * x^4$				
Y_i	PD	DL	SCS	SCB	Q
I	41.37 ± 0.84	37.62 ± 0.83	40.53 ± 1.04	24.02 ± 1.01	43.50 ± 0.86
B_1	27.63 ± 1.78	26.83 ± 1.76	27.70 ± 2.19	14.93 ± 2.14	32.25 ± 1.82
B_2	−15.97 ± 2.51	−15.72 ± 2.49	−18.43 ± 3.10	−14.42 ± 3.02	−16.44 ± 2.58
B_3	1.60 ± 1.83	1.55 ± 1.82	1.30 ± 2.27	5.76 ± 2.21	−0.60 ± 1.88
B_4	10.30 ± 1.71	11.27 ± 1.70	11.98 ± 2.11	14.16 ± 2.05	10.21 ± 1.75
RSS	64.22	63.32	98.00	92.85	67.60
R-Square (COD)	0.99	0.99	0.99	0.99	0.99
Adj. R-Square R^2	0.99	0.99	0.99	0.99	0.99

Y_i-Percentage of passers, RSS-Residual Sum of Squares, I-Intercept, X-corresponding sieve diameter.

The residual sum of squares (RSS), also known as the sum of squares of estimated errors (SSE), is the sum of the squares of the residuals. It measures the deviation between the data and an estimation model, such as a linear regression. A low RSS indicates a good fit between the model and the data, which is a criterion of optimality for the selection of mathematical models. Given that the segregation of the PD model in each of the samples was justified by the variability of the data, its lower CBR values (69.5% and 73.5%) with a high imbibition rate (PD = 2.29%) and its high RSS (64.22%), it can be excluded as a model for controlling granular segregation. The DL model, which gives the best mechanical properties and the lowest RSS (63.32%) of the five models, best controls the granular segregation of 0/31.5 crushed aggregates, particularly in comparison with the SCS model from the same group, which has a higher RSS (98.00%). This is justified by the fact that the PD and SCS models deviate from the reference limits only between the 0.5 mm and 2 mm sieves, which correspond to the coarse sand zone, compared to the DL model (Figure 8). Based on these analyses, the equation derived from the DL can be used to correct particle size distribution curves with high segregation and to define the optimal intervals for representing a sample with no or low segregation

4. Conclusions

The objective of this work was to evaluate the possibilities of generating granular segregation of 0/31.5 crushed aggregates used in road construction in order to minimize their impact on the quality of structures. Based on five sampling models, it was found that the particle size distribution curves diverged from each other, with extremes for the SCB model (only 27.54% fine particles). Analysis of the curve descriptors (Cu, Cc and Mf) shows that TVC 0/31.5 is prone to granular segregation. The PD model produces more variable data than the other models. The DL model, with 44.54% fines and 37.16% gravel, produces a particle size curve that complies with the normative range and is the best at minimizing the effects of segregation in the material. The density and porosity values are higher in the Q and SCB models, favoring water saturation rates above 0.66%, which adversely affects the long-term bearing capacity of the structure. Despite its low intergranular porosity imbibition rates, the bearing capacity of the SCS model is good for a road base layer (CBR between 99% and 103%). It should be noted that materials exhibit granular segregation when they are rich in:

- Fine elements with high intergranular porosity promote a decrease in bearing capacity (case of the Q model).
- Coarse elements with high intergranular porosity increase bearing capacity values (case of the SCB model).

DL modeling provides a multiple linear regression equation capable of correcting segregation grain size curves and controlling crushed aggregates. The application of this model in quarries or on construction road sites consists of verifying the percent passing by of the different fractions that make up the material. The use of full-scale samplers facilitates these operations for adjusting the material stacking.

The next step in this work will focus on validating the DL model experimentally. The implementation of a numerical model to predict the mechanical effects of segregation on granular materials will also be the subject of future research.

In practical terms, the recommendations arising from this study concern the quality control of crushed rock aggregates during the operational phase, namely:

- Control of grain size distribution during production and before use (Cu, Cc and Mf),
- Control of densities and intergranular porosity.

Acknowledgements

Civil Engineering Laboratory of the Higher Polytechnic National School (ENSP) at Marien Ngouabi University.

Conflicts of Interest

The authors declare no conflicts of interest regarding the publication of this paper.

References

[1] Williams, J.C. (1976) The Segregation of Particulate Materials. a Review. *Powder Technology*, **15**, 245-251. https://doi.org/10.1016/0032-5910(76)80053-8

[2] Tuğrul, A. and Zarif, I.H. (1999) Correlation of Mineralogical and Textural Characteristics with Engineering Properties of Selected Granitic Rocks from Turkey. *Engineering Geology*, **51**, 303-317. https://doi.org/10.1016/s0013-7952(98)00071-4

[3] Voivret, C., Radjaï, F., Delenne, J. and El Youssoufi, M.S. (2007) Space-Filling Properties of Polydisperse Granular Media. *Physical Review E*, **76**, Article ID: 021301.

https://doi.org/10.1103/physreve.76.021301

[4] Miskovsky, K., Taborda Duarte, M., Kou, S.Q. and Lindqvist, P. (2004) Influence of the Mineralogical Composition and Textural Properties on the Quality of Coarse Aggregates. *Journal of Materials Engineering and Performance*, **13**, 144-150. https://doi.org/10.1361/10599490418334

[5] Rothenburg, L. and Bathurst, R.J. (1989) Analytical Study of Induced Anisotropy in Idealized Granular Materials. *Géotechnique*, **39**, 601-614. https://doi.org/10.1680/geot.1989.39.4.601

[6] Azéma, E., Radjaï, F., Peyroux, R. and Saussine, G. (2007) Force Transmission in a Packing of Pentagonal Particles. *Physical Review E*, **76**, Article ID: 011301. https://doi.org/10.1103/physreve.76.011301

[7] Dawson, A. (2016) Construction, Quality Control & Performance of Unbound Granular Layers. Chair, TRB Committee AFP70 "Aggregates" 2016.

[8] Boudjedra, F., Benouis, A. and Grini, A. (2020) Effet de la composition sur la ségrégation des bétons. *Academic Journal of Civil Engineering*, **34**, 679-686.

[9] Al-Oraimi, S.K., Taha, R. and Hassan, H.F. (2006) The Effect of the Mineralogy of Coarse Aggregate on the Mechanical Properties of High-Strength Concrete. *Construction and Building Materials*, **20**, 499-503. https://doi.org/10.1016/j.conbuildmat.2004.12.005

[10] Mauduit, V., Mauduit, C., Vulcano-Greullet, N., Coulon, N., Hammoum, F., Kerzreho, J.P., Piau, J.M. and Chabot, A. (2013) Sudden Degradation of Asphalt Pavements during Freeze/Thaw Cycles: Field Case Analysis and Exploratory Laboratory Research.

[11] Panesar, D.K. and Shindman, B. (2012) The Effect of Segregation on Transport and Durability Properties of Self Consolidating Concrete. *Cement and Concrete Research*, **42**, 252-264. https://doi.org/10.1016/j.cemconres.2011.09.011

[12] Cunningham, C.N., Evans, T.M. and Tayebali, A.A. (2013) Gradation Effects on the Mechanical Response of Crushed Stone Aggregate. *International Journal of Pavement Engineering*, **14**, 231-241. https://doi.org/10.1080/10298436.2012.690518

[13] Bilodeau, J. and Doré, G. (2012) Relating Resilient Behaviour of Compacted Unbound Base Granular Materials to Matrix and Interlock Characteristics. *Construction and Building Materials*, **37**, 220-228. https://doi.org/10.1016/j.conbuildmat.2012.07.036

[14] Hydzik-Wiśniewska, J., Wilk, A., Bednarek, Ł. and OIesiak, S. (2018) Mixture of Crushed- Stone Aggregate as Material for Substructure Layers. *Studia Geotechnica et Mechanica*, **40**, 154-162. https://doi.org/10.2478/sgem-2018-0014

[15] Wu, W., Tu, Z., Zhu, Z., Zhang, Z. and Lin, Y. (2019) Effect of Gradation Segregation on Mechanical Properties of an Asphalt Mixture. *Applied Sciences*, **9**, Article 308. https://doi.org/10.3390/app9020308

[16] Mirghasemi, A.A., Rothenburg, L. and Matyas, E.L. (2002) Influence of Particle Shape on Engineering Properties of Assemblies of Two-Dimensional Polygon-Shaped Particles. *Géotechnique*, **52**, 209-217. https://doi.org/10.1680/geot.2002.52.3.209

[17] Ndinga Okina, S., Ahouet, L., Taillandier, F. and Ounina, D. (2024) Influence of the Addition of Palm Kernel Shell and Ash on Concrete Performances: Study of Correlations between Intrinsic Material Properties. *Advanced Materials Research*, **1180**, 115-130. https://doi.org/10.4028/p-4wf9hw

[18] NF EN 932-1 (1996) Tests to Determine the General Properties of Aggregates-Part 1: Sampling Methods.

[19] Elenga, B.D.B., Ahouet, L. and Okina, S.N. (2023) Relationship between the Intrinsic Properties of Sands and the Parameters of Mathematical Particle Size Distribution Models for Predicting Geotechnical Quantities. *Saudi Journal of Civil Engineering*, **7**, 260-273. https://doi.org/10.36348/sjce.2023.v07i10.003

[20] Kennedy, T.W., Tahmoressi, M., Holmgreen Jr., R.J. and Anagnos, J.N. (1986) Segregation in Asphalt Mixtures Produced in Drum Mix Plants Research Project 3-9-84-366. Center for Transportation Research Bureau of Engineering Research, The University of Texas at Austin.

[21] Ferreira, T.R., Luz, J.A.M.D. and Castro, M.H.D. (2022) Live Volume of Conical Stockpile Reclaimed by Gravity. *Research*, *Society and Development*, **11**, e13511628908. https://doi.org/10.33448/rsd-v11i6.28908

[22] NF P 94-056 (1996) French Standard. Soils: Recognition and Tests. Granulometric Analysis. Method by Dry Sieving after Washing, French Standards Association, 5-15.

[23] NF EN 933-2 (2020) Tests to Determine the Geometric Characteristics of Aggregates-Part 2: Determination of Granularity-Test Sieves, Nominal Aperture Sizes.

[24] NF EN 1097-3 (1998) Tests to Determine the Mechanical and Physical Characteristics of Aggregates-Part 3: Method for Determining Bulk Density and Intergranular Porosity.

[25] EN 1097-6 (2022) Tests to Determine the Mechanical and Physical Characteristics of Aggregates-Part 6: Determination of Bulk Density and Water Absorption Coefficient

[26] NF P94-093 (2014) French Standard. Soils: Reconnaissance and Testing-Determining the Compaction References of a Material-Normal Proctor Test-Modified Proctor Test.

[27] NF P94-078 (1997) French Standard: Soils: Reconnaissance and Tests-CBR Index after Immersion-Immediate CBR Index-Immediate Bearing Index-Measurement on Compacted Sample in the CBR Mould.

[28] NF EN 13286-47 (2021) Treated and Untreated Mixtures with Hydraulic Binders-Part 47: Test Methods for Determining the California Bearing Ratio (CBR), Immediate Bearing Ratio (IPI) and Linear Swelling.

[29] C.E.B.T.P. (1984) Practical Guide to Pavement Design for Tropical Countries. French Ministry of Cooperation.

[30] NF EN 13285 (2018) European Standard: Untreated Gravel-Specifications Untreated Gravel-Specifications.

[31] Okina, S.N., Ahouet, L. and Etou, D.G. (2023) Evaluation of Concrete Performances Based Recycled Aggregates of Road and Build Demolition for a Formal Using in the Republic of Congo. *Saudi Journal of Engineering and Technology*, **8**, 267-273. https://doi.org/10.36348/sjet.2023.v08i11.001

[32] Khelalfa, H. (2006) Soil Treatment by Vibroflottation—Application to Protection Structures of DjenDjen Port, Jijel, Algeria. *Journal of Materials and Engineering Structures*, **3**, 149-160.